Inorg. Chem. **2002**, *41*, 818–826

$[Fe(bipy)(CN)_4]^-$ as a Versatile Building Block for the Design of Heterometallic Systems: Synthesis, Crystal Structure, and Magnetic Properties of $PPh_4[Fe^{III}(bipy)(CN)_4]\cdot H_2O$, $[\{Fe^{III}(bipy)(CN)_4\}_2M^{II}(H_2O)_4]\cdot 4H_2O$, and $[\{Fe^{III}(bipy)(CN)_4\}_2Zn^{II}]\cdot 2H_2O$ [bipy = 2,2′-Bipyridine; M = Mn and Zn]

Rodrigue Lescouëzec,[1a] Francesc Lloret,[1a] Miguel Julve,*[,1a] Jacqueline Vaissermann,[1b] and Michel Verdaguer*[,1b]

Departament de Química Inorgànica/Instituto de Ciencia Molecular, Facultat de Química de la Universitat de València, Dr. Moliner 50, 46100-Burjassot, València, Spain, and Laboratoire de Chimie Inorganique et Matériaux Moléculaires, Unité CNRS 7071, Université Pierre et Marie Curie, 4 Place Jussieu, Case 42, 75252 Paris Cedex 05, France

Received July 24, 2001

The new cyano complexes of formulas $PPh_4[Fe^{III}(bipy)(CN)_4]\cdot H_2O$ (**1**), $[\{Fe^{III}(bipy)(CN)_4\}_2M^{II}(H_2O)_4]\cdot 4H_2O$ with M = Mn (**2**) and Zn (**3**), and $[\{Fe^{III}(bipy)(CN)_4\}_2Zn^{II}]\cdot 2H_2O$ (**4**) [bipy = 2,2′-bipyridine and PPh_4 = tetraphenylphosphonium cation] have been synthesized and structurally characterized. The structure of complex **1** is made up of mononuclear $[Fe(bipy)(CN)_4]^-$ anions, tetraphenyphosphonium cations, and water molecules of crystallization. The iron(III) is hexacoordinated with two nitrogen atoms of a chelating bipy and four carbon atoms of four terminal cyanide groups, building a distorted octahedron around the metal atom. The structure of complexes **2** and **3** consists of neutral centrosymmetric $[\{Fe^{III}(bipy)(CN)_4\}_2M^{II}(H_2O)_4]$ heterotrinuclear units and crystallization water molecules. The $[Fe(bipy)(CN)_4]^-$ entity of **1** is present in **2** and **3** acting as a monodentate ligand toward $M(H_2O)_4$ units [M = Mn(II) (**2**) and Zn(II) (**3**)] through one cyanide group, the other three cyanides remaining terminal. Four water molecules and two cyanide nitrogen atoms from two $[Fe(bipy)(CN)_4]^-$ units in trans positions build a distorted octahedron surrounding Mn(II) (**2**) and Zn(II) (**3**). The structure of the $[Fe(phen)(CN)_4]^-$ complex ligand in **2** and **3** is close to that of the one in **1**. The intramolecular Fe–M distances are 5.126(1) and 5.018(1) Å in **2** and **3**, respectively. **4** exhibits a neutral one-dimensional polymeric structure containing two types of $[Fe(bipy)(CN)_4]^-$ units acting as bismonodentate (Fe(1)) and trismonodentate (Fe(2)) ligands versus the divalent zinc cations through two *cis*-cyanide (Fe(1)) and three *fac*-cyanide (Fe(2)) groups. The environment of the iron atoms in **4** is distorted octahedral as in **1**–**3**, whereas the zinc atom is pentacoordinated with five cyanide nitrogen atoms, describing a very distorted square pyramid. The iron–zinc separations across the single bridging cyanides are 5.013(1) and 5.142(1) Å at Fe(1) and 5.028(1), 5.076(1), and 5.176(1) Å at Fe(2). The magnetic properties of **1**–**3** have been investigated in the temperature range 2.0–300 K. **1** is a low-spin iron(III) complex with an important orbital contribution. The magnetic properties of **3** correspond to the sum of two magnetically isolated spin triplets, the antiferromagnetic coupling between the low-spin iron(III) centers through the –CN–Zn–NC– bridging skeleton (iron–iron separation larger than 10 Å) being very weak. More interestingly, **2** exhibits a significant intramolecular antiferromagnetic interaction between the central spin sextet and peripheral spin doublets, leading to a low-lying spin quartet.

Introduction

The use of the hexacyanometalate unit $[B(CN)_6]^{q-}$ as a complex toward totally hydrated metal ions $[A(H_2O)_6]^{p+}$ (A and B are transition-metal ions) has provided a large family of three-dimensional compounds known as Prussian blue analogues which exhibit very interesting spectroscopic, magnetic, and magnetooptical properties.[2−15] The two most

* To whom correspondence should be addressed. E-mail: miguel.julve@uv.es.

(1) (a) Universitat de València. (b) Université Pierre et Marie Curie.

10.1021/ic0107882 CCC: $22.00
Published on Web 01/25/2002

exciting results of this research activity are (i) the preparation of molecule-based magnets with critical temperatures (T_c) as high as 376[5] and 315 K[15] and (ii) the achievement of photoinduced magnetization upon light irradiation on Prussian blue analogues[9,10] and also on lower dimensional cyanide-bridged bimetallic assemblies containing a light-sensitive complex as the building block.[11−14]

If the Prussian blue analogues present exciting magnetic properties, single crystals of these highly insoluble three-dimensional complexes are hardly obtained. Furthermore, vacancies and channels accommodate guest molecules,[16,17] which makes difficult both the determination of the crystallographic structure and the interpretation of the magnetic behavior of these three-dimensional magnetic systems. To overcome some of these problems, a highly rewarding synthetic strategy has been widely used which consists of reacting the hexacyanometalate unit with the coordinatively unsaturated complex $[A(L)_x(H_2O)_y]^{p+}$, L being a neutral or anionic polydentate ligand.[18] Apart from a few examples of high-spin penta- and heptanuclear complexes with ground spin states up to 27/2,[19,20] this strategy has provided one-, two- and three-dimensional cyanide-bridged bimetallic networks as the main products, the dimensionality being strongly dependent on the charges of the A- and B-containing units and the number and relative positions of the coordinated water molecules of A.[18] These results show that the preparation of discrete cyano-bridged polynuclear species would require a decrease of the number of cyano groups on the B precursor. A few results have been reported in this respect in bioinorganic,[21] organometallic,[22,23] and magnetostructural[24−26] studies. So, the monocyano building block of formula [Fe(OEP)(py)(CN)] (OEP = octaethylporphyrinate dianion and py = pyridine) was used to prepare heterobimetallic complexes containing the $Fe^{III}-CN-Cu^{II}$ unit to mimic the iron−copper binuclear site in cyanide-inhibited cytochrome *c* oxidase and terminal quinol oxidases.[21] A new class of organometallic solids with cyanide as a bridge (trinuclear species, cages, and helical chains) have been reported recently, the mononuclear cyano precursors being [Cp*(dppe)Fe(CN)],[22] [Cp*(PPh_3)$_2$Ru(CN)],[22] and [Cp*(M(CN)$_3$)]$^-$ (M = Ir and Rh).[23] Very recently, nice discrete cluster analogues of the cubic cages existing in the Prussian blue type structure such as the 14-metal, $[(Me_3tacn)_8Cr_8Ni_6(CN)_{24}]^{12+}$, and 19-metal, $[(Me_3tacn)_{10}Cr_{10}Ni_9(CN)_{42}]^{6+}$, assemblies ($Me_3$tacn = *N*,*N*′,*N*″-trimethyl-1,4,7-triazacyclononane) were prepared when the neutral [(Me_3tacn)Cr((CN)$_3$] mononuclear complex was allowed to react with hydrated metal ions.[24b] Finally, the dicyano[25] and tetracyano[26] low-spin iron(III) complexes of formulas $[Fe(bipy)_2(CN)_2]^+$ (bipy = 2,2′-bipyridine) and $[Fe(phen)(CN)_4]^-$ (phen = 1,10-phenanthroline) allowed the preparation of the cyanide-bridged cyclic tetranuclear complex $[Fe_2(bipy)_4(CN)_4Cu_2(bipy)_2]^{6+}$ and the isostructural double zigzag chains $[\{Fe(phen)(CN)_4\}_2M(H_2O)_2]\cdot 4H_2O$ with M = Mn and Zn. A quintet spin ground state occurs in the tetranuclear compound because of the intramolecular ferromagnetic interaction between the Fe(III) and Cu(II) local spin doublets, whereas the intrachain antiferromagnetic coupling between the Fe(III) (spin doublet) and Mn(II) (spin sextuplet) leads to ferrimagnetic behavior.

In an effort to continue this remarkably diverse chemistry starting from a tailored cyanometalate molecular precursor, we explored the use of the new low-spin iron(III) complex $[Fe(bipy)(CN)_4]^-$ as a ligand. Our first results presented here concern the preparation and crystal structure of the precursor

(2) Fehlhammer, W. P.; Fritz, M. *Chem. Rev.* **1993**, *93*, 1243 and references therein.
(3) Dunbar, K. M.; Heintz, R. A. *Prog. Inorg. Chem.* **1997**, *45*, 283 and references therein.
(4) Verdaguer, M.; Bleuzen, A.; Marvaud, V.; Vaissermann, J.; Seuleiman, M.; Desplanches, C.; Scuiller, A.; Train, C.; Garde, R.; Gelly, G.; Lomenech, C.; Rosenman, I.; Veillet, R.; Cartier, C.; Villain, F. *Coord. Chem. Rev.* **1999**, *190*−*192*, 1023 and references therein.
(5) Holmes, S. M.; Girolami, G. S. *J. Am. Chem. Soc.* **1999**, *121*, 5593 and references therein.
(6) Hatlevik, O.; Buchamann, W. E.; Zhang, J.; Manson, J. L.; Miller, J. S. *Adv. Mater.* **1999**, *11*, 914.
(7) (a) Sra, A. K.; Andruh, M.; Kahn, O.; Golhen, S.; Ouahab, L.; Yakhmi, J. V. *Angew. Chem., Int. Ed. Engl.* **1999**, *38*, 2606. (b) Larionova, J.; Kahn, O.; Golhen, S.; Ouahab, L.; Clérac, R.; Bartolomé, J.; Burriel, R. *Mol. Cryst. Liq. Cryst.* **1999**, *334*, 651.
(8) Buschmann, W. E.; Miller, J. S. *Inorg. Chem.* **2000**, *39*, 2411.
(9) (a) Sato, O.; Einaga, A.; Fujishima, A.; Hashimoto, K. *Inorg. Chem.* **1999**, *38*, 4405. (b) Sato, O.; Iyoda, T.; Fujishima, A.; Hashimoto, K. *Science* **1996**, *271*, 49.
(10) (a) Bleuzen, A.; Lomenech, C.; Escax, V.; Villain, F.; Varret, F.; Cartier dit Moulin, C.; Verdaguer, M. *Inorg. Chem.* **2000**, 6648. (b) Cartier dit Moulin, C.; Villain, F.; Bleuzen, A.; Arrio, M. A.; Sainctavit, P.; Lomenech, C.; Escax, V.; Baudelet, F.; Dartyge, E.; Gallet, J. J.; Verdaguer, M. *Inorg. Chem.* **2000**, *122*, 6653.
(11) (a) Sra, A. K.; Rombaut, G.; Lahitête, F.; Golhen, S.; Ouahab, L.; Mathonière, C.; Yakhmi, J. V.; Kahn, O. *New J. Chem.* **2000**, *24*, 871. (b) Rombaut, G.; Golhen, S.; Ouahab, L.; Mathonière, C.; Kahn, O. *J. Chem. Soc., Dalton Trans.* **2000**, 3609. (c) Rombaut, G.; Verelst, M.; Golhen, S.; Ouahab, L.; Mathonière, C.; Kahn, O. *Inorg. Chem.* **2001**, *40*, 1151.
(12) (a) Waltz, W. L.; Adamson, A. W. *J. Phys. Chem.* **1969**, *73*, 4250. (b) Waltz, W. L.; Adamson, A. W.; Fleischauer, P. D. *J. Am. Chem. Soc.* **1967**, *89*, 3923. (c) Shirom, M.; Siderer, Y. *J. Chem. Phys.* **1972**, *57*, 1013. (d) Shirom, M.; Siderer, Y. *J. Chem. Phys.* **1972**, *58*, 1250. (e) Vogler, A.; Losse, W.; Kunkely, H. *J. Chem. Soc., Chem. Commun.* **1979**, 187. (f) Bettelheim, A.; Shirom, M. *Chem. Phys. Lett.* **1971**, *9*, 166.
(13) (a) Gu, Z.; Sato, O.; Iyoda, T.; Hashimoto, K.; Fujishima, A. *J. Phys. Chem.* **1996**, *47*, 18289. (b) Gu, Z.; Sato, O.; Iyoda, T.; Hashimoto, K.; Fujishima, A. *Chem. Mater.* **1997**, *9*, 1092.
(14) Clemente-León, M.; Coronado, E.; Galán-Mascarós, J. R.; Gómez-García, C. J.; Woike, Th.; Clemente-Juan, J. M. *Inorg. Chem.* **2001**, *40*, 87.
(15) Ferlay, S.; Mallah, T.; Ouahès, R.; Veillet, P.; Verdaguer, M. *Science* **1995**, *378*, 701.
(16) Lüdi, A.; Güdel, H. U. *Struct. Bonding (Berlin)* **1973**, *14*, 1.
(17) Reference 2, pp 323−325.
(18) Ohba, M.; Okawa, H. *Coord. Chem. Rev.* **2000**, *198*, 313 and references therein.
(19) (a) Mallah, T.; Auberger, C.; Verdaguer, M.; Veillet, P. *J. Chem. Soc., Chem. Commun.* **1995**, 61. (b) Scuiller, A.; Mallah, T.; Nivorozkhin, A.; Verdaguer, M.; Veillet, P. *New J. Chem.* **1996**, 1.
(20) (a) Langenberg, K. V.; Batten, S. R.; Berry, K. J.; Hockless, D. C. R.; Moubaraki, B.; Murray, K. S. *Inorg. Chem.* **1997**, *36*, 5006. (b) Marvilliers, A.; Pei, Y.; Boquera, J. C.; Vostrikova, K.; Paulsen, C.; Rivière, E.; Audière, J.-P.; Mallah, T. *Chem. Commun.* **1999**, 1951.
(21) (a) Scott, M. J.; Lee, S. C.; Holm, R. H. *Inorg. Chem.* **1994**, *33*, 4651. (b) Scott, M. J.; Holm, R. H. *J. Am. Chem. Soc.* **1994**, *116*, 11357.
(22) Chen, Z. N.; Appelt, R.; Vahrenkamp, H. *Inorg. Chim. Acta* **2000**, *309*, 65.
(23) (a) Klausmeyer, K. K.; Scott, R. W.; Rauchfuss, T. B. *J. Am. Chem. Soc.* **1999**, *121*, 2705. (b) Contakes, S. M.; Klausmeyer, K. K.; Rauchfuss, T. B. *Inorg. Chem.* **2000**, *39*, 2069.
(24) (a) Heinrich, J. L.; Berseth, P. A.; Long, J. R. *Chem. Commun.* **1998**, 1231. (b) Sokol, J. J.; Shores, M. P.; Long, J. R. *Angew. Chem.* **2001**, *113*, 242.
(25) Oshio, H.; Tamada, O.; Onodera, H.; Ito, T.; Ikoma, T.; Tero-Kubota, S. *Inorg. Chem.* **1999**, *38*, 5686.
(26) Lescouëzec, R.; Lloret, F.; Julve, M.; Vaissermann, J.; Verdaguer, M.; Llusar, R.; Uriel, S. *Inorg. Chem.* **2001**, *40*, 2065.

Table 1. Crystallographic Data for $PPh_4[Fe^{III}(bipy)(CN)_4]\cdot H_2O$ (**1**), $[\{Fe^{III}(bipy)(CN)_4\}_2M^{II}(H_2O)_4]\cdot 4H_2O$ with M = Mn (**2**) and Zn (**3**), and $[\{Fe^{III}(bipy)(CN)_4\}_2Zn^{II}]\cdot 2H_2O$ (**4**)

	1	**2**	**3**	**4**
empirical formula	$C_{38}H_{30}FePN_6O$	$C_{28}H_{32}Fe_2MnN_{12}O_8$	$C_{28}H_{32}Fe_2ZnN_{12}O_8$	$C_{28}H_{20}Fe_2ZnN_{12}O_2$
fw	673.5	831.2	841.7	733.6
space group	$P2_1/c$	$P2_1/n$	$P2_1/n$	$P2_1/n$
a, Å	12.013(4)	6.620(7)	6.499(6)	19.872(4)
b, Å	19.888(8)	19.134(4)	19.155(5)	7.242(3)
c, Å	14.486(6)	14.319(4)	14.338(4)	20.776(4)
β, deg	100.70(3)	93.90(5)	93.32(5)	96.47(2)
V, Å^3	3400(2)	1809(2)	1781(2)	2971(2)
Z	4	2	2	4
λ, Å	0.71069	0.71069	0.71069	0.71069
ρ_{calcd}, g cm^{-3}	1.31	1.53	1.57	1.64
T, °C	22	22	22	22
μ(Mo Kα), cm^{-1}	5.26	11.8	15.5	18.3
R[a]	0.0830	0.0591	0.0441	0.0460
R_w[b]	0.0926	0.0693	0.0512	0.0527

[a] $R = \sum||F_o| - |F_c||/\sum|F_o|$. [b] $R_w = [\sum w(|F_o| - |F_c|)^2/\sum wF_o^2]^{1/2}$. $w = w'[1 - ((|F_o| - |F_c|)/6\sigma(F_o))^2]^2$, where $w' = 1/\sum_r A_r T_r(X)$ with three coefficients for a Chebyshev series (4.46, −1.37, and 2.91 for **1**, 5.65, −0.712, and 4.28 for **2**, 4.58, −1.61, and 3.47 for **3**, and 4.39, −0.608, and 3.32 for **4**) for which $X = F_c/F_c(\max)$.

complex $PPh_4[Fe^{III}(bipy)(CN)_4]\cdot H_2O$ (**1**) and its derivatives $[\{Fe^{III}(bipy)(CN)_4\}_2M^{II}(H_2O)_4]\cdot 4H_2O$ with M = Mn (**2**) and Zn (**3**) and $[\{Fe^{III}(bipy)(CN)_4\}_2Zn^{II}]\cdot 2H_2O$ (**4**) [bipy = 2,2′-bipyridine and PPh_4 = tetraphenylphosphonium cation] and the investigation of the magnetic properties of **1**−**3**.

Experimental Section

Materials. Chemicals were purchased from commercial sources as reagents pure for analysis and used as received. $K_2[Fe^{II}(bipy)(CN)_4]\cdot 3H_2O$ was prepared as described in the literature.[27] Elemental analysis (C, H, N) was performed by the Microanalitycal Service of the Universidad Autónoma de Madrid. The values of the Fe:P (**1**), Fe:Mn (**2**), and Fe:Zn (**3** and **4**) molar ratios 1:1 (**1**), 2:1 (**2**), and 2:1 (**3** and **4**) were determined by electron microscopy at the Servei de Microscopia Electrònica de la Universitat de València.

Syntheses. $PPh_4[Fe^{III}(bipy)(CN)_4]\cdot H_2O$ (1). Chlorine gas was bubbled through a warm dark red aqueous solution (200 mL) of $K_2[Fe^{II}(bipy)(CN)_4]\cdot 3H_2O$ (4 mmol, 1.80 g) for 1/2 h under continuous stirring. A color change from red to orange was observed. The addition of a concentrated warm aqueous solution (20 mL) of tetraphenylphosphonium chloride (4 mmol, 1.50 g) caused the precipitation of complex **1** as an orange solid. Recrystallization in acetonitrile afforded X-ray-quality prismatic orange crystals of **1**. Yield: 2.15 g, 80%. Anal. Calcd for $C_{38}H_{30}FeN_6OP$ (**1**): C, 67.80; H, 4.46; N, 12.45. Found: C, 67.63; H, 4.41; N, 12.50. IR stretching cyanide (KBr)/cm^{-1}: 2118m.

$[\{Fe^{III}(bipy)(CN)_4\}_2Mn^{II}(H_2O)_4]\cdot 4H_2O$ (2). The slow addition of solid lithium perchlorate (0.2 mmol, 22 mg) to an acetonitrile solution (20 mL) of complex **1** (0.2 mmol, 135 mg) caused the precipitation of $Li[Fe^{III}(bipy)(CN)_4]$ as an orange crystalline solid. The solid was dissolved in 20 mL of water, and the resulting orange solution was mixed with an aqueous solution (20 mL) containing manganese(II) nitrate tetrahydrate (0.1 mmol, 26 mg). Red platelike crystals of **2** were separated from the resulting red solution by slow evaporation at room temperature. The yield was practically quantitative. Anal. Calcd for $C_{28}H_{32}Fe_2MnN_{12}O_8$ (**2**): C, 40.47; H, 3.85; N, 20.22. Found: C, 40.21; H, 3.74; N, 20.3. IR stretching cyanide (KBr)/cm^{-1}: 2151m and 2117m.

$[\{Fe^{III}(bipy)(CN)_4\}_2Zn^{II}(H_2O)_4]\cdot 4H_2O$ (3) and $[\{Fe^{III}(bipy)(CN)_4\}_2Zn^{II}]\cdot 2H_2O$ (4). The preparation of complexes **3** and **4** was carried out using a procedure similar to that employed for complex **2**. Zinc(II) nitrate hexahydrate (0.1 mmol, 30 mg) was used as the zinc source. Two types of crystals were obtained by slow evaporation of the final solution containing a 1:1 Fe:Zn molar ratio: orange needles of **3** as the main product (49 mg) and only a few red prisms of **4**. The overall yield was about 60%. This relatively low yield compared to the parent manganese system is due to the formation of an unidentified iron−zinc cyano polymer which is insoluble in common solvents. The formula of complex **4** was determined by X-ray diffraction on single crystals. Anal. Calcd for $C_{28}H_{32}Fe_2ZnN_{12}O_8$ (**3**): C, 39.97; H,3.80; N, 19.97. Found: C, 39.85; H, 3.74; N, 19.83. IR stretching cyanide (KBr)/cm^{-1}: 2167m and 2119m (**3**) and 2171m and 2157m (**4**).

Physical Measurements. The IR spectra of **1**−**4** (KBr pellets) were recorded with a Bruker IF S55 spectrophotometer. Magnetic susceptibility measurements on polycrystalline samples of **1**−**3** were carried out with a Quantum Design SQUID magnetometer in the temperature range 2.0−300 K and under an applied magnetic field of 0.1 T. The magnetic study of complex **4** was not carried out because of the very small amount of this complex that we obtained. Diamagnetic corrections of the constituent atoms were estimated from Pascal constants[28] as -405×10^{-6} (**1**), -452×10^{-6} (**2**), and -453×10^{-6} (**3**) cm^3 mol^{-1}.

X-ray Data Collection and Structure Refinement. Crystals of dimensions 0.04 × 0.20 × 0.32 (**1**), 0.20 × 0.32 × 0.65 (**2**), 0.10 × 0.20 × 0.80 (**3**), and 0.05 × 0.10 × 0.60 (**4**) mm were mounted on an Enraf-Nonius CAD-4 diffractometer and used for data collection. Diffraction data were collected at room temperature by using graphite-monochromated Mo Kα radiation (λ = 0.71069 Å) with the $\omega-2\theta$ method. Accurate cell dimensions and orientation matrixes were obtained by least-squares refinements of 25 accurately centered reflections with $8.0° < \theta < 9.0°$ (**1**) and $12.0° < \theta < 12.5°$ (**2**−**4**). No significant variations were observed in the intensities of two checked reflections during data collections. The data were corrected for Lorentz and polarization effects. An empirical correction was performed by the use of DIFABS[29] (**1** and **2**) or the ψ-scan curve (**3** and **4**). The maximum and minimum transmission factors were 1 and 0.87 for **1**, 1 and 0.95 for **2**, 1 and 0.88 for **3**, and 1 and 0.91 for **4**. Information concerning the crystallographic data collections and structure refinements is summarized in Table 1. Of the 3511 (**1**), 3581 (**2**), 3923 (**3**), and

(27) Schilt, A. A. *J. Am. Chem. Soc.* **1960**, *82*, 3000.

(28) Earnshaw, A. *Introduction to Magnetochemistry*; Academic Press: London, 1968.

(29) Walker, N.; Stuart, D. *Acta Crystallogr.* **1983**, *A39*, 156.

Table 2. Selected Bond Lengths (Å) and Angles (deg)[a,b] for **1**

Fe(1)−N(11)	1.98(2)	Fe(1)−N(12)	2.00(2)
Fe(1)−C(1)	1.87(2)	Fe(1)−C(2)	1.89(3)
Fe(1)−C(3)	1.90(2)	Fe(1)−C(4)	1.91(2)
C(1)−N(1)	1.14(2)	C(2)−N(2)	1.16(3)
C(3)−N(3)	1.17(2)	C(4)−N(4)	1.15(2)
N(11)−Fe(1)−N(12)	80.2(8)	N(11)−Fe(1)−C(1)	96.4(9)
N(12)−Fe(1)−C(1)	176.3(9)	N(11)−Fe(1)−C(2)	176.2(9)
N(12)−Fe(1)−C(2)	96.1(10)	C(1)−Fe(1)−C(2)	87.3(10)
N(11)−Fe(1)−C(3)	90.8(8)	N(12)−Fe(1)−C(3)	92.1(8)
C(1)−Fe(1)−C(3)	86.6(9)	C(1)−Fe(1)−C(2)	88.8(9)
N(11)−Fe(1)−C(4)	89.8(8)	N(12)−Fe(1)−C(4)	91.0(9)
C(1)−Fe(1)−C(4)	90.3(10)	C(2)−Fe(1)−C(4)	90.8(10)
C(3)−Fe(1)−C(4)	176.9(10)	Fe(1)−C(1)−N(1)	174.9(22)
Fe(1)−C(2)−N(2)	172.6(23)	Fe(1)−C(3)−N(3)	174.4(20)
Fe(1)−C(4)−N(4)	177.2(20)		
Hydrogen Bonds			
O(1)···N(1a)	2.981(28)	O(1)···N(2b)	2.835(27)

[a] Estimated standard deviations in the last significant digits are given in parentheses. [b] Symmetry code: (a) $1 + x$, $1/2 - y$, $1/2 + z$; (b) $1 + x$, y, $1 + z$.

5851 (**4**) measured reflections in the θ ranges 1−20° (**1**) and 1−25° (**2**−**4**) with index ranges $0 \le h \le 11$, $0 \le k \le 19$, and $-13 \le l \le \mp 13$ (**1**), $0 \le h \le 7$, $0 \le k \le 22$, and $-16 \le l \le \mp 16$ (**2**), $0 \le h \le 8$, $0 \le k \le 23$, and $-17 \le l \le \mp 17$ (**3**), and $0 \le h \le 23$, $0 \le k \le 8$, and $-24 \le l \le \mp 24$ (**4**), 3182 (**1**), 3167 (**2**), 3479 (**3**), and 5219 (**4**) were unique. From these, 955 (**1**), 1799 (**2**) 1635 (**3**), and 2825 (**4**) were observed [$I > 2\sigma(I)$ (**1**) and $I > 3\sigma(I)$ (**2**−**4**)] and used for the refinement of the structures.

The structures were solved by direct methods through SHELX-86[30] and subsequently refined by Fourier recycling. For **1**, all atoms were isotropically refined and the phenyl rings were refined as rigid bodies. All non-hydrogen atoms for **2**−**4** were refined anisotropically. All hydrogen atoms (except those of the water molecules) were introduced in calculated positions and were allocated one overall isotropic thermal parameter. The final full-matrix least-squares refinement on F through the PC version of CRYSTALS[31] reached convergence with values of the R and R_w indices listed in Table 1, the number of variables being 142 (**1**), 233 (**2** and **3**), and 407 (**4**). The residual maxima and minima in the final Fourier difference maps were 0.41 and 0.49 e Å^{-3} for **1**, 0.94 and −0.63 e Å^{-3} for **2**, 0.62 and −0.36 e Å^{-3} for **3**, and 0.99 and −0.73 e Å^{-3} for **4**. The values of the goodness-of-fit were 1.11 (**1**), 1.13 (**2** and **4**), and 1.14 (**3**). Selected interatomic bond distances and angles are given in Tables 2 (**1**), 3 (**2**), 4 (**3**), and 5 (**4**).

Results and Discussion

Description of the Structures. PPh$_4$[Fe^{III}(bipy)(CN)$_4$]·H$_2$O (1). The structure of compound **1** consists of mononuclear [Fe(bipy)(CN)$_4$]$^-$ anions (Figure 1), tetraphenylphosphonium cations, and water molecules of crystallization which are linked by electrostatic forces, hydrogen bonds, and van der Waals interactions.

Each iron(III) cation is coordinated by two bipy nitrogen atoms and four cyanide carbon atoms, taking a distorted octahedral geometry. The short bite of chelating bipy [80.2-(8)° for N(11)−Fe(1)−N(12)] is one of the main factors accounting for this distortion. The values of the Fe(1)−N(bipy) bonds in **1** [1.98(2) and 2.00(2) Å] are the same as those found in the low-spin iron(II) K$_2$[Fe^{II}(bipy)(CN)$_4$]·2.5H$_2$O [1.987(4)−2.003(4) Å][32] and iron(III) [Fe^{III}(bipy)$_2$(CN)$_2$]ClO$_4$ [1.954(4)−1.993(5) Å][33] complexes. Good agreement is observed between the Fe(1)−C(cyano) bond distances

Table 3. Selected Bond Lengths (Å) and Angles (deg)[a,b] for **2**

Fe(1)−N(11)	1.971(5)	Fe(1)−N(12)	1.984(5)
Fe(1)−C(1)	1.911(7)	Fe(1)−C(2)	1.911(7)
Fe(1)−C(3)	1.960(7)	Fe(1)−C(4)	1.950(7)
Mn(1)−O(1)	2.185(3)	Mn(1)−O(2)	2.212(7)
Mn(1)−N(1)	2.183(6)	C(1)−N(1)	1.149(9)
C(2)−N(2)	1.142(9)	C(3)−N(3)	1.126(8)
C(4)−N(4)	1.124(9)		
N(11)−Fe(1)−N(12)	81.2(2)	N(11)−Fe(1)−C(1)	97.5(2)
N(12)−Fe(1)−C(1)	178.6(2)	N(11)−Fe(1)−C(2)	177.6(3)
N(12)−Fe(1)−C(2)	96.7(3)	C(1)−Fe(1)−C(2)	84.6(3)
N(11)−Fe(1)−C(3)	90.2(2)	N(12)−Fe(1)−C(3)	88.4(2)
C(1)−Fe(1)−C(3)	91.3(3)	C(2)−Fe(1)−C(3)	88.5(3)
N(11)−Fe(1)−C(4)	90.7(2)	N(12)−Fe(1)−C(4)	90.6(2)
C(1)−Fe(1)−C(4)	89.8(3)	C(2)−Fe(1)−C(4)	90.6(3)
C(3)−Fe(1)−C(4)	178.5(3)	Fe(1)−C(1)−N(1)	174.2(6)
Fe(1)−C(2)−N(2)	177.6(8)	Fe(1)−C(3)−N(3)	177.2(6)
Fe(1)−C(4)−N(4)	177.8(6)	O(1)−Mn(1)−O(2)	92.3(3)
O(1)−Mn(1)−O(2a)	87.7(3)	O(1)−Mn(1)−N(1)	88.0(2)
O(1)−Mn(1)−N(1a)	92.0(2)	O(2)−Mn(1)−N(1)	91.9(3)
O(2)−Mn(1)−N(1a)	88.1(3)	Mn(1)−N(1)−C(1)	159.5(6)
Hydrogen Bonds			
O(1)···O(11)	2.415(23)	O(1)···N(2b)	2.779(9)
O(2)···O(10)	2.769(9)	O(10)···N(3c)	2.869(8)
O(10)···N(4d)	2.795(9)	O(10)···O(11)	2.921(20)

[a] Estimated standard deviations in the last significant digits are given in parentheses. [b] Symmetry code: (a) $-x$, $-y$, $-z$; (b) $1 - x$, $-y$, $-z$; (c) $-1/2 + x$, $-1/2 - y$, $-1/2 + z$; (d) $-1 + x$, y, z.

Table 4. Selected Bond Lengths (Å) and Angles (deg)[a,b] for **3**

Fe(1)−N(11)	1.976(5)	Fe(1)−N(12)	1.980(5)
Fe(1)−C(1)	1.913(7)	Fe(1)−C(2)	1.909(6)
Fe(1)−C(3)	1.948(7)	Fe(1)−C(4)	1.929(7)
Zn(1)−O(1)	2.097(5)	Zn(1)−O(2)	2.169(5)
Zn(1)−N(1)	2.082(5)	C(1)−N(1)	1.132(9)
C(2)−N(2)	1.145(8)	C(3)−N(3)	1.124(8)
C(4)−N(4)	1.131(8)		
N(11)−Fe(1)−N(12)	81.2(2)	N(11)−Fe(1)−C(1)	98.6(2)
N(12)−Fe(1)−C(1)	179.6(2)	N(11)−Fe(1)−C(2)	177.1(2)
N(12)−Fe(1)−C(2)	95.9(2)	C(1)−Fe(1)−C(2)	84.3(3)
N(11)−Fe(1)−C(3)	90.8(2)	N(12)−Fe(1)−C(3)	88.2(2)
C(1)−Fe(1)−C(3)	91.4(3)	C(2)−Fe(1)−C(3)	88.7(3)
N(11)−Fe(1)−C(4)	89.9(2)	N(12)−Fe(1)−C(4)	90.4(2)
C(1)−Fe(1)−C(4)	90.0(3)	C(2)−Fe(1)−C(4)	90.4(3)
C(3)−Fe(1)−C(4)	178.3(3)	Fe(1)−C(1)−N(1)	175.5(6)
Fe(1)−C(2)−N(2)	178.2(6)	Fe(1)−C(3)−N(3)	176.6(5)
Fe(1)−C(4)−N(4)	178.6(6)	O(1)−Zn(1)−O(2)	93.7(2)
O(1)−Zn(1)−O(2a)	86.3(2)	O(1)−Zn(1)−N(1)	87.6(2)
O(1)−Zn(1)−N(1a)	92.4(2)	O(2)−Zn(1)−N(1)	92.3(2)
O(2)−Zn(1)−N(1a)	87.7(2)	Zn(1)−N(1)−C(1)	159.0(6)
Hydrogen Bonds			
O(1)···O(11)	2.682(8)	O(1)···N(2)	2.811(8)
O(2)···O(10)	2.846(7)	O(10)···N(3c)	2.875(8)
O(10)···N(4d)	2.779(8)	O(10)···O(11)	2.785(8)

[a] Estimated standard deviations in the last significant digits are given in parentheses. [b] Symmetry code: (a) $-x$, $-y$, $-z$; (b) $1 - x$, $-y$, $-z$; (c) $-1/2 + x$, $-1/2 - y$, $-1/2 + z$; (d) $-1 + x$, y, z.

(30) (a) Sheldrick, G. M. *SHELX-86: Program for Crystal Structure Solution*; University of Göttingen: Göttingen, Germany, 1986. (b) Watkin, D. J.; Prout, C. K.; Pearce, L. J. C. Crystallography Laboratory, University of Oxford, Oxford, U.K., 1996.
(31) Watkin, D. J.; Prout, C. K.; Carruthers, J. R.; Betteidge, P. W. *CRYSTALS*; Chemical Crystallography Laboratory, University of Oxford: Oxford, U.K., 1996; Issue 10.
(32) Nieuwenhuyzen, M.; Bertram, B.; Gallagher, J. F.; Vos, J. G. *Acta Crystallogr.* **1998**, *C54*, 603.
(33) Lu, T.-H.; Kao, H.-Y.; Wu, D. I.; Kong, K. C.; Cheng, C. H. *Acta Crystallogr.* **1988**, *C44*, 1184.

Table 5. Selected Bond Lengths (Å) and Angles (deg)[a,b] for **4**

Fe(1)−N(11)	1.974(5)	Fe(1)−N(12)	1.976(5)
Fe(1)−C(1)	1.882(7)	Fe(1)−C(3)	1.950(7)
Fe(1)−C(4)	1.896(7)	Fe(1)−C(5)	1.932(7)
Fe(2)−N(21)	1.974(5)	Fe(2)−N(22)	1.977(5)
Fe(2)−C(2)	1.908(6)	Fe(2)−C(6)	1.950(6)
Fe(2)−C(7)	1.930(6)	Fe(2)−C(8)	1.911(7)
Zn(1)−N(1)	2.121(6)	Zn(1)−N(2)	1.997(5)
Zn(1)−N(3b)	2.074(6)	Zn(1)−N(6c)	2.113(5)
Zn(1)−N(8d)	2.048(6)	C(1)−N(1)	1.150(8)
C(2)−N(2)	1.135(8)	C(3)−N(3)	1.135(8)
C(4)−N(4)	1.152(8)	C(5)−N(5)	1.134(8)
C(6)−N(6)	1.130(8)	C(7)−N(7)	1.141(8)
C(8)−N(8)	1.133(8)		
N(11)−Fe(1)−N(12)	80.8(2)	N(11)−Fe(1)−C(1)	96.9(3)
N(12)−Fe(1)−C(1)	172.0(2)	N(11)−Fe(1)−C(3)	91.9(2)
N(12)−Fe(1)−C(3)	96.6(2)	C(1)−Fe(1)−C(3)	91.2(3)
N(11)−Fe(1)−C(4)	176.6(3)	N(12)−Fe(1)−C(4)	95.9(3)
C(1)−Fe(1)−C(4)	86.5(3)	C(3)−Fe(1)−C(4)	88.5(3)
N(11)−Fe(1)−C(5)	90.4(2)	N(12)−Fe(1)−C(5)	87.2(2)
C(1)−Fe(1)−C(5)	85.2(3)	C(3)−Fe(1)−C(5)	175.9(3)
C(4)−Fe(1)−C(5)	89.4(3)	N(21)−Fe(2)−N(22)	81.0(2)
N(21)−Fe(2)−C(2)	177.3(2)	N(22)−Fe(2)−C(2)	96.4(2)
N(21)−Fe(2)−C(6)	90.1(2)	N(22)−Fe(2)−C(6)	97.4(2)
C(2)−Fe(2)−C(6)	89.4(3)	N(21)−Fe(2)−C(7)	90.7(2)
N(22)−Fe(2)−C(7)	86.9(2)	C(2)−Fe(2)−C(7)	90.0(3)
C(6)−Fe(2)−C(7)	175.7(3)	N(21)−Fe(2)−C(8)	95.6(2)
N(22)−Fe(2)−C(8)	171.2(2)	C(2)−Fe(2)−C(8)	87.0(3)
C(6)−Fe(2)−C(8)	90.7(2)	C(7)−Fe(2)−C(8)	85.0(3)
Fe(1)−N(11)−C(11)	124.5(5)	Fe(1)−N(11)−C(15)	114.8(4)
Fe(1)−N(12)−C(16)	114.2(5)	Fe(1)−N(12)−C(20)	126.8(5)
Fe(2)−N(21)−C(21)	126.2(4)	Fe(2)−N(21)−C(25)	114.4(4)
Fe(2)−N(22)−C(26)	113.8(4)	Fe(2)−N(22)−C(30)	125.5(4)
Fe(1)−C(1)−N(1)	175.4(6)	Fe(2)−C(2)−N(2)	178.8(5)
Fe(1)−C(3)−N(3)	174.7(6)	Fe(1)−C(4)−N(4)	178.6(7)
Fe(1)−C(5)−N(5)	178.4(6)	Fe(2)−C(6)−N(6)	175.1(6)
Fe(2)−C(7)−N(7)	179.2(6)	Fe(2)−C(8)−N(8)	175.0(6)
N(1)−Zn(1)−N(2)	99.9(2)	N(1)−Zn(1)−N(3b)	89.3(2)
N(2)−Zn(1)−N(3b)	107.3(2)	N(1)−Zn(1)−N(6c)	161.0(2)
N(2)−Zn(1)−N(6c)	98.9(2)	N(3b)−Zn(1)−N(6c)	87.6(2)
N(1)−Zn(1)−N(8d)	84.2(2)	N(2)−Zn(1)−N(8d)	105.5(2)
N(3b)−Zn(1)−N(8d)	147.2(2)	N(6c)−Zn(1)−N(8d)	88.3(2)
Zn(1)−N(1)−C(1)	154.3(6)	Zn(1)−N(2)−C(2)	172.7(5)
Zn(1e)−N(3)−C(3)	173.9(5)	Zn(1d)−N(6)−C(6)	173.0(5)
Zn(1b)−N(8)−C(8)	173.2(6)		

[a] Estimated standard deviations in the last significant digits are given in parentheses. [b] Symmetry code: (b) $x, -1 + y, z$; (c) $1/2 - x, -1/2 + y, 1/2 - z$; (d) $1/2 - x, 1/2 + y, 1/2 - z$; (e) $x, 1 + y, z$.

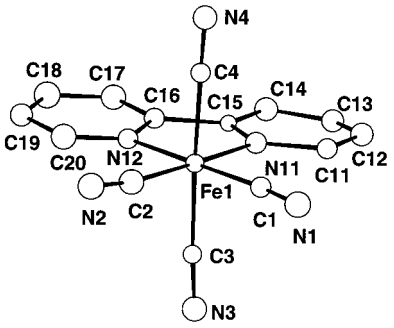

Figure 1. Perspective drawing of the mononuclear $[Fe(bipy)(CN)_4]^-$ unit of complex **1** showing the atom numbering. Thermal ellipsoids are drawn at the 30% probability level.

of **1** [1.87(2)−1.91(2) Å] and those reported for other cyano-containing mononuclear low-spin iron(III) [1.906(8)−1.95-(1) Å][26,33] and iron(II) [1.891(5)−1.936(5) Å][32,34] complexes. Nevertheless, the occurrence of the tetraphenylphosphonium cation in the structure and the magnetic moment of **1** (see below) unambiguously reveal a low-spin iron(III) species. The cyanide stretching frequency in the infrared spectrum of **1**, which appears as a medium-intensity peak at 2118 cm^{-1} (single peak at 2120 cm^{-1} for $PPh_4[Fe^{III}(phen)(CN)_4]\cdot 2H_2O$ and $[Fe(bipy)_2(CN)_2]ClO_4$) provides additional evidence of this low-spin iron(III) character.

The bipy ligand as a whole is close to planarity, the dihedral angle between the two planar pyridyl rings being ca. 5°. Bond lengths and angles within the bipy ligand are in agreement with those reported for the free bipy molecule.[35] The C(1)C(2)N(11)N(12)Fe(1) set of atoms defining a five-membered chelate at the metal atom is coplanar, the largest deviation from their mean plane being 0.0016 Å at the iron atom. Although the separation between the mean planes of two bipy ligands from adjacent $[Fe(bipy)(CN)_4]^-$ units is ca. 3.5 Å, they are so slipped that no graphitic-like interaction may be considered. The bond lengths and angles involving the cyanide ligands compare well with those found in other cyano-containing low-spin mononuclear iron(III) complexes.[26,33,36] The iron atom and each cyanide are almost in a line [values for Fe−C−N ranging from 172.6(23)° to 177.2(20)°]. The bulky tetraphenylphosphonium cation exhibits the expected tetrahedral shape, and its bond lengths and angles are as expected. Interestingly, the PPh_4^+ cations are grouped by pairs exhibiting the sextuple phenyl embrace type interaction[37] with an intrapair P···P distance of ca. 6.20 Å. Regular alternating layers of PPh_4^+ cations and $[Fe(bipy)(CN)_4]^-$ anions occur in the unit cell (Figure S1 in the Supporting Information). In addition, two of the four cyanide groups and the water molecule are involved in hydrogen-bonding interactions with donor−acceptor distances of less than 3.0 Å (see the end of Table 2), leading to a chain of water-linked $[Fe(bipy)(CN)_4]^-$ units along the z axis (Figure S2). The shortest intermolecular iron−iron separation is 7.840(6) Å [Fe(1)···Fe(1c); (c) $1 - x, -y, -z$].

$[\{Fe^{III}(bipy)(CN)_4\}_2M^{II}(H_2O)_4]\cdot 4H_2O$ (M = Mn (2) and Zn (3)). **2** and **3** are isostructural compounds whose structure is made up of centrosymmetric neutral trinuclear entities of formula $[\{Fe^{III}(bipy)(CN)_4\}_2M^{II}(H_2O)_4]$ where the $[Fe(phen)(CN)_4]^-$ unit acts as a monodentate ligand through one of its four cyanide groups toward a central $[M(H_2O)_4]^{2+}$ motif with M = Mn (**1**) and Zn (**3**) (Figure 2). Four water molecules of crystallization contribute to the stabilization of the lattice by hydrogen-bonding interactions which involve the coordinated water molecules and three of the four cyanide groups (see the end of Tables 3 and 4).

As in **1**, each iron atom in **2** and **3** is coordinated by two bipy nitrogen atoms and four cyanide carbon atoms, in a distorted octahedral geometry. The values of the Fe−N(bipy) bonds and that of the angle subtended at the iron atom by the chelating bipy are very close to those found in **1**. The Fe(1)−C bond lengths in **2** and **3** are equal within error to those found in **1**. The values of the two Fe−C(cyano) bonds

(34) Zhan, S.; Meng, Q.; You, X.; Wang, G.; Zheng, P. J. *Polyhedron* **1996**, *15*, 2665.

(35) Merrit, L. L.; Schroeder, E. D. *Acta Crystallogr.* **1956**, *9*, 801.
(36) Vannerberg, N. G. *Acta Chem. Scand.* **1972**, *26*, 2863.
(37) Dance, I.; Scudder, M. *Chem.—Eur. J.* **1996**, *2*, 481 and references therein.

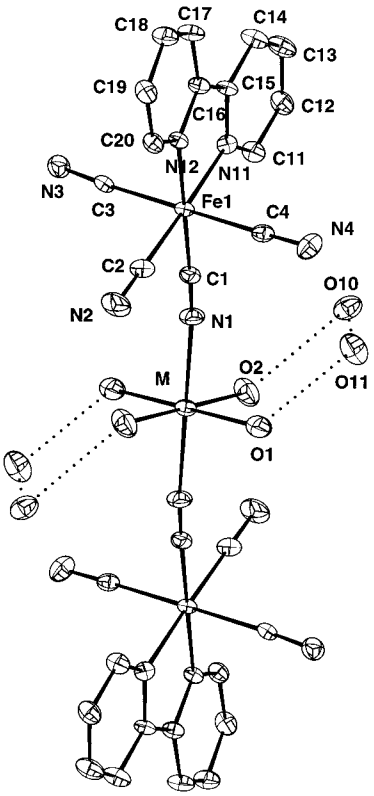

Figure 2. Perspective drawing of the structure of the trinuclear species [{Fe^{III}(bipy)(CN)$_4$}$_2$M^{II}(H$_2$O)$_4$]·4H$_2$O (M = Mn (**2**) and Zn (**3**)) along with the atom numbering. Thermal ellipsoids are drawn at the 30% probability level. Hydrogen bonds between the water molecules are illustrated by broken lines.

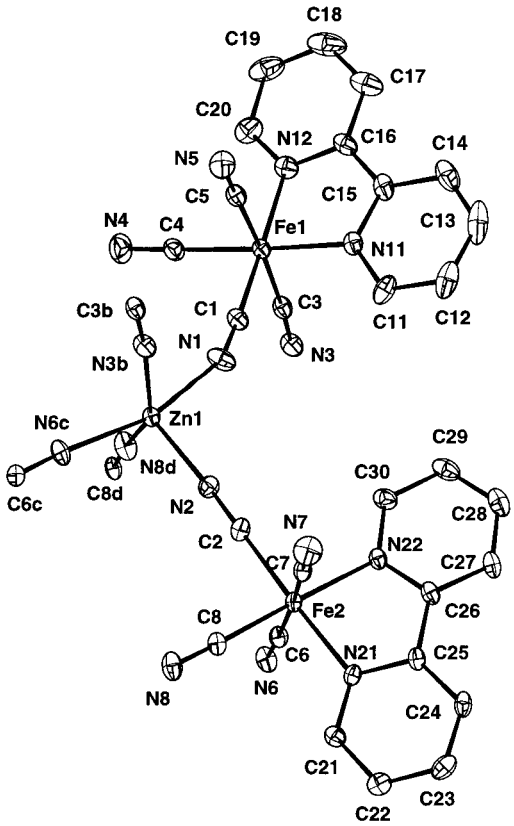

Figure 3. Perspective drawing of the crystallographically independent unit of **4** showing the cyanide bridges and the atom numbering. Thermal ellipsoids are drawn at the 30% probability level.

corresponding to the cyano groups coordinated in trans positions to each other are slightly longer than those in the cis-coordinated ones. The Fe−C−N angles for both terminal (177.2(6)−177.8(6)° in **2** and 176.6(5)−178.6(6)° in **3**) and bridging (174.2(6)° in **1** and 175.5(6)° in **3**) cyanide groups are somewhat bent, their deviations from strict linearity comparing well with those observed in the parent bimetallic double chains [{Fe^{III}(phen)(CN)$_4$}$_2$M^{II}(H$_2$O)$_2$]·4H$_2$O (M = Mn and Zn).[26] The manganese (**2**) and zinc (**3**) atoms are hexacoordinated with two cyanide nitrogen atoms in trans positions and four water molecules, building a distorted MN$_2$O$_4$ octahedral surrounding. The values of the angle M−N(1)−C(1) [159.5(6)° (M = Mn) and 150.0(6)° (M = Zn)] depart significantlty from 180°. The occurrence of two peaks of medium intensity in the CN stretching region of the IR spectra of **2** and **3** is consistent with the presence of bridging and terminal cyanide ligands.

The chelating bipy ligand is quasi-planar, the dihedral angle between the planes of its two pyridyl rings being ca. 4° (**2**) and 5° (**3**). The five-membered chelate Fe(1)N(11)C(15)C(16)N(12) is practically planar [the largest deviation from the mean plane is 0.014 Å (**2**) and 0.007 Å (**3**) for Fe(1)]. The trinuclear units of **2** and **3** in the unit cell are well isolated from each other (Figure S3). Although the shortest intermolecular bipy−bipy contact is ca. 3.52 Å (**2**) and 3.51 Å (**3**) along the *x* axis (Figure S4), a weak overlap between the bipy mean planes occurs because of their large slipping.

The values of the intramolecular Fe(1)···M separation through bridging cyanide are 5.126(1) Å [Fe(1)···Mn(1)] and 5.018(1) Å [Fe(1)···Zn(1)], whereas the shortest intermolecular metal−metal distances are 6.620(1) Å (**2**) and 6.499(1) Å (**3**) [Fe(1)···Fe(1d) and Fe(1)···Fe(1e); (e) $-1 + x, y, z$], 8.601(2) Å (**2**) and 8.697(2) Å (**3**) [Fe(1)···Fe(1f); (f) $-x, -y, 1 - z$], and 8.654(2) Å (**2**) and 8.756(2) Å (**3**)] [Fe(1)···Fe(1g); (g) $1 - x, -y, -1 - z$].

[{Fe^{III}(bipy)(CN)$_4$}$_2$Zn^{II}]·2H$_2$O (4). The structure of complex **4** is made up of neutral one-dimensional [{Fe^{III}(bipy)(CN)$_4$}$_2$Zn^{II}] units running parallel to the *b* axis and crystallization water molecules which are held together by van der Waals interactions. The crystallographically independent unit contains two types of iron atoms (Fe(1) and Fe(2)) and one zinc atom (Zn(1)) (see Figure 3), the latter being connected to five iron atoms through cyanide bridges. The [{Fe^{III}(bipy)(CN)$_4$}$_2$Zn^{II}] motif (see Figure 4) builds a corrugated ladder-like chain with regular alternating Fe(2) and Zn(1) atoms along the edges, each rung being defined by an iron−zinc pair. In addition, each pair of adjacent zinc atoms are connected through another iron atom (Fe(1)). A single cyano group bridges each iron−zinc pair.

The two crystallographically independent iron atoms (Fe(1) and Fe(2)) exhibit the same distorted octahedral FeN$_2$C$_4$ surrounding observed in **1**−**3**. The difference between [Fe(1)(bipy)(CN)$_4$]$^-$ and [Fe(2)(bipy)(CN)$_4$]$^-$ is that the former acts as a bismonodentate ligand toward the zinc atoms through two (cis positions) of its four cyanide groups, whereas the latter adopts a trismonodentate coordination

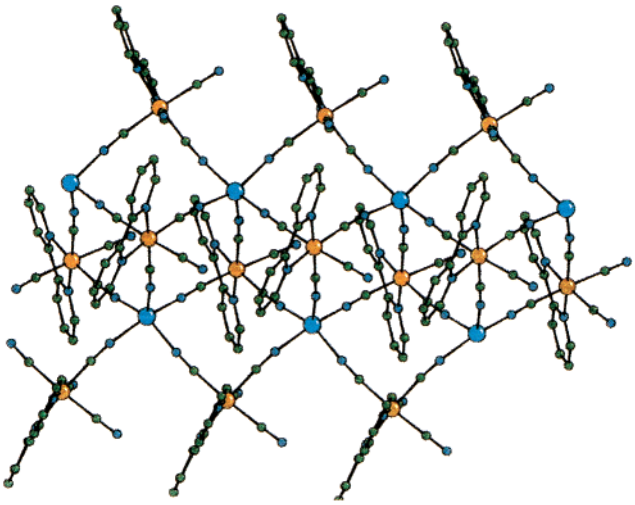

Figure 4. A view of a fragment of the structure of **4** along the *b* axis. The metal atoms are represented as orange (Fe) and blue (Zn) circles, and the crystallization water molecules have been omitted for clarity.

Chart 1

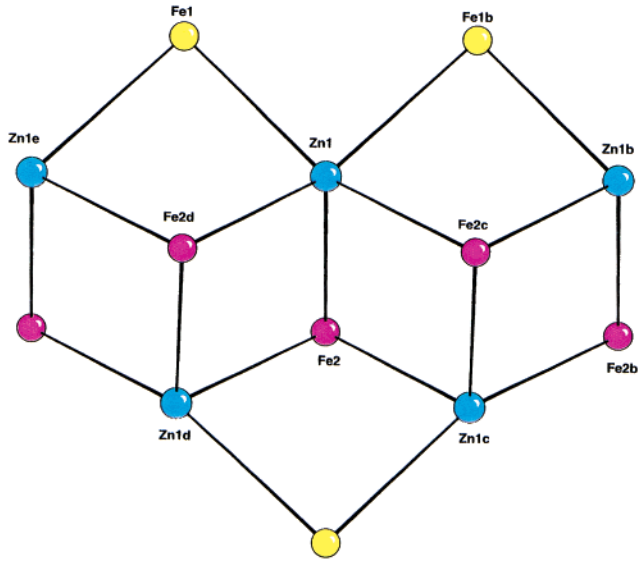

mode (three cyanides in fac positions), only one of its four cyanide groups being terminal. As in **1**−**3**, the values of the two Fe−C(cyano) bonds corresponding to the two trans-coordinated cyano groups at the Fe(1) and Fe(2) atoms are significantly longer than those in the cis-coordinated ones. The Fe−C−N angles for both terminal [178.4(6)° and 178.6(7)° (Fe(1)) and 179.2(6)° (Fe(2))] and bridging [174.7(6)° and 175.4(6)° (Fe(1)) and 175.0(6)°, 175.1(6)°, and 178.8(5)° (Fe(2))] cyanide groups are bent. The zinc atom is pentacoordinated with five cyanide nitrogen atoms, forming a severely distorted ZnN_5 square pyramid. The deviations from the mean basal plane are ±0.12 Å, the zinc atom being shifted by 0.46 Å from this mean plane toward the apical N(2) atom. All the values of the Zn−N−C bond depart from linearity, but whereas four of them vary in a narrow range somewhat below 180° [172.7(5)−173.9(5) Å], the remaining one is highly bent [154.3(6)° for Zn(1)−N(1)−C(1)]. The C−N bond lengths for terminal and bridging C−N ligands are in agreement with those observed in **3**. The IR spectrum of **4** provides spectral evidence of the occurrence of bridging (doublet at 2171 and 2157 cm^{-1}) and terminal (single peak at 2124 cm^{-1}) cyanide ligands.

The dihedral angle between the planes of the two pyridyl rings of the bipy group coordinated to Fe(1) is ca. 2° (7° in that bound to Fe(2)). The five-membered chelates Fe(1)N(11)C(15)C(16)N(12) and Fe(2)N(21)C(25)C(26)N(22) are quasi-planar, the largest deviation from the mean planes being 0.07 Å at Fe(1). The large separation (7.24 Å) between the parallel quasi-eclipsed bipy ligands along the *b* axis precludes any significant intrachain $\pi-\pi$ interaction (Figure 4). Weak interchain bipy−bipy contacts are observed, the separation between the significantly slipped bipy ligands of neighboring $[Fe(bipy)(CN)_4]^-$ units being 3.8 Å (Figure S5). The value of the dihedral angle between adjacent mean planes of the corrugated ladder-like motif is 90° (angle at the Fe(2)···Zn(1) hinge in Chart 1), whereas those between the Fe(1)Zn(1e)Zn(1)Fe(2d) mean plane and Fe(2d)Zn(1d)Fe(2)Zn(1) and Fe(2e)Zn(1e)Fe(2d)Zn(1d) mean planes are 99° and 80°. The values of the iron−zinc distances though bridging cyanide are 5.013(1) [Fe(1)···Zn(1)], 5.142(1) [Fe(1)···Zn(1e)], 5.028(1) [Fe(2)···Zn(1)], 5.076(1) [Fe(2)···Zn(1c)], and 5.176(1) Å [Fe(2)···Zn(1d)]. The remaining intrachain iron−iron and zinc−zinc separations are 7.242(1) [Fe(1)···Fe(1b), Fe(2)···Fe(2b) and Zn(1)···Zn(1e)], 6.662(1) [Fe(1)···Fe(2d)], 8.468(1) [Fe(1)···Fe(2)], 8.485(1) [Fe(1)···Fe(2e)], 7.546(1) [Fe(2)···Fe(2d)], and 6.795(1) Å [Zn(1)···Zn(1d)].

Magnetic Properties of 1−3. The temperature dependence of the $\chi_M T$ product for complexes **1** and **3** (χ_M being the magnetic susceptibility per mole of Fe(III)) is shown in Figure 5. $\chi_M T$ for **1** monotonically decreases from 0.71 cm^3 mol^{-1} K at room temperature to 0.53 cm^3 mol^{-1} K at 1.9 K. The value of μ_{eff} (ca. 2.38 μ_B) at room temperature for **1** agrees with those previously reported for other low-spin iron(III) complexes.[38] It is clearly above the spin-only value for an isolated low-spin iron(III) center (0.375 cm^3 mol^{-1} K for $S = 1/2$ assuming $g_{Fe} = 2.0$) because of the presence of a significant orbital contribution. The variation of $\chi_M T$ versus T for **1** is characteristic of a low-spin octahedral iron(III) system with spin−orbit coupling of the $^2T_{2g}$ ground term.[39−41] The significant distortion of the iron(III) environment in **1** (roughly C_{2v} symmetry around the metal atom) caused by the presence of one bidentate bipy ligand and four terminal cyanide ligands is not enough to totally quench the orbital contribution of the ground state. The $\chi_M T$ versus T plot for **3** matches that of **1** from room temperature to 25 K, as expected due to the fact that the same low-spin iron(III) complex occurs in **1** and **3**. Then, in the low-temperature range, $\chi_M T$ for **3** slightly decreases and attains a value of 0.42 cm^3 mol^{-1} K at 1.9 K. Weak intra- and/or intermolecular antiferromagnetic interactions between the low-spin iron-

(38) Casey, A. T.; Mitra, S. In *Theory and Applications of Molecular Paramagnetism*; Boudreaux, E. A., Mulay, L. N., Eds.; John Wiley and Sons: New York, 1976; Chapter 3, p 191.
(39) Pavlishchuk, V. V.; Koval, I. A.; Goreshnik, E.; Addison, A. W.; van Albada, G. A.; Reedijk, J. *Eur. J. Inorg. Chem.* **2001**, 297.
(40) Patra, A. K.; Ray, M.; Mukherjee, R. *Inorg. Chem.* **2000**, *39*, 652.
(41) Ray, M.; Mukherjee, R.; Richardson, J. F.; Buchanan, R. M. *J. Chem. Soc., Dalton Trans.* **1993**, 2451.

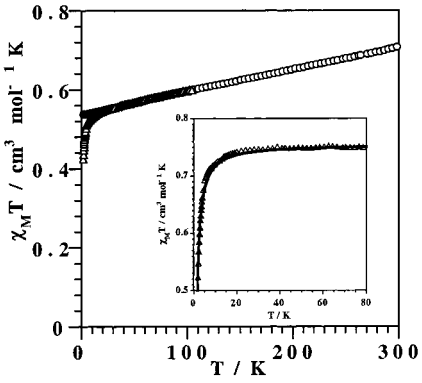

Figure 5. Thermal dependence of the $\chi_M T$ product for complexes **1** (○) and **3** (△). The inset shows the corrected $\chi_M T$ versus T plot for **3** in the low-temperature region (see the text).

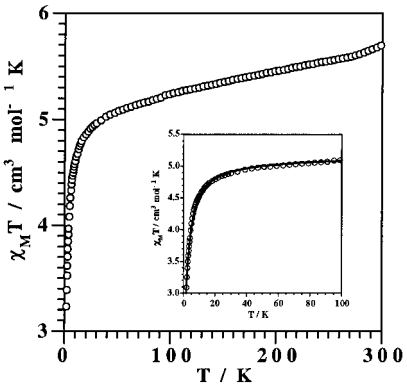

Figure 6. Thermal dependence of the $\chi_M T$ product for complex **2** (○). The inset shows the corrected $\chi_M T$ versus T plot for **2** (see the text).

(III) centers in **3** would account for this decrease. Given that the trimeric units of **3** are well isolated from each other (the shortest intermolecular iron−iron separation is ca. 6.5 Å), the small antiferromagnetic coupling observed would most likely involve the intramolecular Fe(1)−CN−Zn(1)−NC−Fe(1a) exchange pathway. To get a rough estimate of this antiferromagnetic coupling, we have subtracted first the $\chi_M T$ data from **1** from those of **3** (for two iron atoms). Then, 0.75 cm^3 mol^{-1} K (Curie law term per two noninteracting spin doublets with $g = 2.0$) was added to the difference data. The corrected $\chi_M T$ data for $T < 100$ K are shown in the inset of Figure 5. The procedure is expected to rule out the orbital contribution to the magnetic behavior of **3**, and to allow the analysis through a *spin-only* formalism. The corrected $\chi_M T$ data of **3** were treated by the isotropic Hamiltonian $\hat{H} = -J\hat{S}_{Fe1}\cdot\hat{S}_{Fe2}$, which corresponds to a low-spin iron(III) dimer (two interacting local spin doublets with $g_{Fe1} = g_{Fe2} = 2.0$) with J as the exchange coupling parameter. Least-squares fit (solid line in the inset of Figure 5) leads to $J = -1.3$ cm^{-1} with $R = 1.4 \times 10^{-4}$ (R is the agreement factor defined as $\sum_i[(\chi_M T)_{obsd}(i) - (\chi_M T)_{calcd}(i)]^2/[(\chi_M T)_{obsd}(i)]^2$). This small exchange coupling is obtained through a crude approximation and can be considered as an upper limit of the intramolecular antiferromagnetic coupling.

The temperature dependence of the $\chi_M T$ product for complex **2** (χ_M being the magnetic susceptibility per Fe_2Mn unit) is shown in Figure 6. The value of $\chi_M T$ at room temperature is 5.70 cm^3 mol^{-1} K. This value is consistent with the presence of a high-spin Mn(II) atom and two low-spin Fe(III) atoms magnetically isolated. As the temperature is lowered, the $\chi_M T$ product continuously decreases at it reaches a value of 3.20 cm^3 mol^{-1} K at 1.9 K. This value is clearly below that of a magnetically isolated spin sextet (4.375 cm^3 mol^{-1} K for $S = 5/2$ with $g = 2.0$), indicating that a significant antiferromagnetic interaction between the Mn(II) and Fe(III) occurs. This is well visualized in the inset of Figure 6, where we have plotted the difference between the $\chi_M T$ data of **2** and twice those of **1** plus a Curie law term per two noninteracting spin doublets with $g = 2.0$. As done for complex **3** and for lack of a better approach, we analyzed the magnetic data of the inset of Figure 6 through the isotropic Hamiltonian (eq 1),

$$\hat{H} = -J[\hat{S}_{Fe1}\cdot\hat{S}_{Mn} + \hat{S}_{Fe2}\cdot\hat{S}_{Mn}] - j\hat{S}_{Fe1}\cdot\hat{S}_{Fe2} \qquad (1)$$

where J and j are the intramolecular exchange coupling parameters between adjacent and peripheral spin carriers, respectively. A common value of 2.0 was fixed for g_{Mn}, g_{Fe1}, and g_{Fe2}. Least-squares fit (solid line in the inset of Figure 6) leads to the following set of parameters: $J = -0.87$ cm^{-1}, $j = -1.3$ cm^{-1}, and $R = 4.9 \times 10^{-5}$. The fitted values of J and j are correlated. Variations in j slightly affect the J values. A fit obtained with a fixed j value at 0 cm^{-1} results in $J = -0.9$ cm^{-1} with a similar quality of fit.

Several points concerning the nature and magnitude of the computed exchange couplings in **2** and **3** deserve to be commented on. First, the values must be considered with caution because of the crude approach used to estimate them. As they are the first ones to be reported, any comparison is precluded. More experimental data are needed to substantiate them and to establish their dependence on relevant structural parameters such as the bond lengths and the bending at the bridging cyanide. Second, the antiferromagnetic coupling between high-spin Mn(II) and low-spin Fe(III) through bridging cyanide in **2** results from a net overlap of the magnetic orbitals through the π t_{2g}–t_{2g} pathway ($t_{2g}^3e_g^2$ and $t_{2g}^5e_g^0$ configurations for Mn(II) and Fe(III), respectively). Two exchange pathways are particularly efficient, the *xz* and *yz* ones, if one defines the *z* axis along Fe−Mn. The same π t_{2g}–t_{2g} exchange pathway is operative in **3** with only one magnetic orbital per center and leads to an antiferromagnetic coupling (ca. -1.3 cm^{-1}) through the diamagnetic −CN−Zn−CN− bridging skeleton. In both cases, the weak π overlap leads to a small interaction. Third, it is satisfying to find good agreement between the exchange couplings between the peripheral low-spin iron(III) centers in the isostructural trinuclear units of **2** and **3**. Fourth, at first sight it seems surprising that j is larger than J in **3**, the separation between the interacting spins in the former being double that in the latter. This can be understood when taking into account the different numbers of unpaired electrons (n_M) of the interacting centers (five versus one in J and one versus one in j). In fact, the coupling energies to be compared[43] are $n_{Mn}n_{Fe}J$ ($= 5J = -4.5$ cm^{-1}) versus $n_{Fe}n_{Fe}j$ ($= j = -1.3$ cm^{-1}).

(42) Martin, L. L.; Martin, R. L.; Murray, K. S.; Sargeson, A. M. *Inorg. Chem.* **1990**, *29*, 1387.

Let us finish with a brief comment on different products obtained when using $[FeL(CN)_4]^-$ (L = bipy and phen) as a complex toward Mn(II) and Zn(II) (M) ions. In a previous work with the phen-containing precursor, we obtained neutral bimetallic Fe_2M double chains,[26] whereas here, using the bipy derivative, we only obtained the neutral heterotrinuclear Fe_2M compounds and also an unprecedented Fe_2Zn ladder-like compound. Most likely, the insolubility of the neutral trinuclear complexes **2** and **3** would preclude the formation of the double chains observed in the phen case, which require the assembling of the trinuclear units through additional cyano bridges.

In summary, the main results of the present work are the following: (i) a new anionic building block containing cyanide and bipy as ligands has been characterized (complex **1**); (ii) its use as a ligand toward first-row transition-metal ions has been explored, allowing the preparation of the first cyano-bridged trinuclear $Fe^{III}2M^{II}$ species (M = Mn (**2**) and Zn (**3**)) and an unprecedented corrugated ladder-like $Fe^{III}_2Zn^{II}$ compound (**4**); (iii) weak but significant antiferromagnetic interactions between Fe(III) and Mn(II) through bridging cyanide (**2**) and between terminal Fe(III) ions through the −CN−M(II)−NC− pathway [M = Mn (**2**) and Zn (**3**)] are observed and evaluated.

(43) Kahn, O. *Struct. Bonding (Berlin)* **1987**, *68*, 89.

Safety Note. Perchlorate complexes are potentially explosive, and every attempt should be made to substitute anions such as the fluorosulfonates for the perchlorates. We used in our syntheses only small amounts of material, and the perchlorate-containing solids were never heated. The dilute solutions were handled with care and evaporated slowly in an open hood (cf. ref 44).

Acknowledgment. This work was supported by the TMR Program from the European Union (Contract ERBFMRXCT98-0181), the Spanish Dirección General de Investigación Científica y Técnica (DGICYT) (Project PB97-1397), and the European Science Foundation through the Molecular Magnets Programme.

Supporting Information Available: Figures S1−S5 (crystal packing of **1**, hydrogen-bonding pattern in **1**, crystal packing of **2**, bipy−bipy overlap in **2**, and projection of the neutral chains of **4** down the *b* axis) and X-ray crystallographic files in CIF format for complexes **1**−**4**. This material is available free of charge via the Internet at http://pubs.acs.org.

IC0107882

(44) *J. Chem. Educ.* **1973**, *50*, A335; **1985**, *62*, 1001. *Chem. Eng. News* **1983**, *61* (Dec 5), 4; **1963**, *41* (July 8), 47.